Host–Guest Systems Hot Paper

DOI: 10.1002/ange.201408677

Construction of Matryoshka-Type Structures from Supercharged Protein Nanocages**

*Tobias Beck, Stephan Tetter, Matthias Künzle, and Donald Hilvert**

Abstract: *Designing nanoscaled hierarchical structures with increasing levels of complexity is challenging. Here we show that electrostatic interactions between two complementarily supercharged protein nanocages can be effectively utilized to create nested Matryoshka-type structures. Cage-within-cage complexes containing spatially ordered iron oxide nanoparticles spontaneously self-assemble upon mixing positively supercharged ferritin compartments with AaLS-13, a larger shell-forming protein with a negatively supercharged lumen. Exploiting engineered Coulombic interactions and protein dynamics in this way opens up new avenues for creating hierarchically organized supramolecular assemblies for application as delivery vehicles, reaction chambers, and artificial organelles.*

The construction of nested and double-walled structures has received much attention in the fields of supramolecular chemistry and materials science. Such hierarchical assemblies consist of an outer shell, which provides mechanical support as well as separation from the outside environment, and at least one inner shell, which partitions the interior space into compartments that can impart new properties and encapsulate distinct functional molecules. Nested metal–organic frameworks, for instance, have been reported to exhibit enhanced thermal stability and increased gas storage capacity.[1] In another example, ball-in-socket structures, assembled in films from doubly concave aromatic compounds and fullerene derivatives, were used to create novel organic solar cells.[2] In nature, compartmentalization physically links genotype and phenotype, and further enables the simultaneous operation of otherwise incompatible metabolic processes. Self-assembling liposomes, which mimic the phospholipid bilayers of cellular membranes and subcellular organelles, have been extensively exploited as delivery vehicles and molecular reaction chambers.[3]

Proteins are attractive building blocks for the construction of hierarchically ordered nanoscale architectures.[4] The structural and functional diversity of virus particles[5] and bacterial protein-based microcompartments[6] illustrates the functional opportunities made possible by proteins that spontaneously self-assemble into shell-like structures. Studies on encapsulins, natural molecular containers that package different proteins and enzymes,[7] including other nanocages,[8] indicate that short peptide tags can be used to target specific guest molecules to the interior of these self-assembling protein shells. Complementary electrostatic interactions represent a potentially versatile alternative for assembling non-natural supramolecular cage complexes. We recently reported a simple cargo loading system based on the capsid-forming enzyme lumazine synthase from *Aquifex aeolicus* (AaLS). The lumen of AaLS was negatively supercharged through rational design and directed evolution to

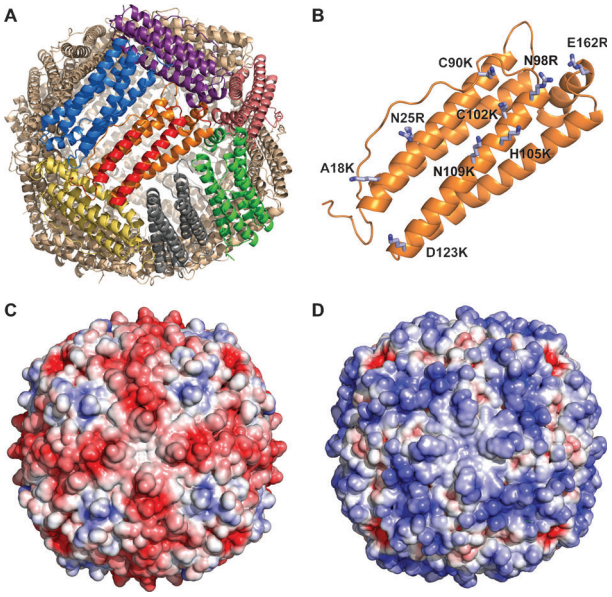

Figure 1. Design of the supercharged ferritin nanocage. A) Human heavy chain ferritin (PDB ID 2CEI) with seven monomers displayed in different colors. Permissible sites for mutation with the Rosetta software are highlighted in red for the central monomer (orange). B) Model, calculated with Rosetta, depicting one monomer of supercharged FtnQC12 in orange [same orientation as in (A)] and the nine mutations that were introduced in gray. C) Electrostatic potential mapped onto the solvent-accessible surface of wtFtn. View along one fourfold symmetry axis. D) Electrostatic potential mapped onto the solvent-accessible surface of FtnQC12. Red: $-5\ kTe^{-1}$, blue: $+5\ kTe^{-1}$.

[*] Dr. T. Beck, S. Tetter, M. Künzle, Prof. Dr. D. Hilvert
Laboratory of Organic Chemistry, ETH Zürich
8093 Zürich (Switzerland)
E-mail: hilvert@org.chem.ethz.ch

[**] We thank Maja Günthert, Stephan Handschin, Dr. Miriam Lucas and Dr. Alla Sologubenko at the Electron Microscopy Facility of ETH Zürich (ScopeM), Dr. Eita Sasaki for help with electron microscopy measurements, and Reinhard Zschoche for providing wtAaLS. This work was generously supported by the ETH Zürich and the European Research Council under the European Union's Seventh Framework Program (FP/2007–2013)/ERC Grant Agreement number ERC-AdG-2012-321295 (to D.H.). T.B. gratefully acknowledges the Marie Curie Action within the FP7-PEOPLE program (IEF-2011-299400) for funding.

Supporting information for this article is available on the WWW under http://dx.doi.org/10.1002/anie.201408677.

afford the variant AaLS-13, which efficiently packages positively charged protein cargo through complementary Coulombic interactions both in vivo and in vitro.[9] In the current study, we show that the dynamic properties of this system can also be exploited to create nested cage-within-cage (Matryoshka-type) structures.

As a guest, we chose human heavy chain ferritin, a protein nanocage involved in iron mineralization and storage.[10] Ferritin is composed of 24 monomers (Figure 1A) that assemble into an octahedrally symmetric capsid with a diameter of approximately 12 nm.[11] In principle, the lumen of AaLS-13, which has an inner diameter of about 25 nm,[9b,12] should accommodate up to four such particles.[13] To facilitate efficient packaging in the negatively charged interior of AaLS-13 capsids, we re-engineered the exterior surface of wild-type ferritin (wtFtn). Positively supercharged variants were designed with the Rosetta software,[14] as previously described for supercharged antibodies,[15] by introducing arginine and lysine residues at multiple sites on the exterior surface of the capsid. The variant FtnQC12 (Figure 1B) contains nine additional cationic residues per monomer (Figure S1 in the Supporting Information) and a calculated electrostatic potential that is highly positive owing to the +264 increase in net theoretical charge per cage (Figure 1C versus 1D).

FtnQC12 was readily produced in *E. coli* in yields similar to those for wtFtn (see the Supporting Information). Treatment with DNase and RNase, followed by ammonium sulfate precipitation and ion exchange chromatography, ensured complete removal of nucleic acids bound to the positively charged surface. The protein obtained by this protocol exhibited high purity (Figure S2A) and was soluble in low salt buffers. Further analysis by size-exclusion column chromatography and circular dichroism spectroscopy confirmed that it assembles as a nanocage with similar size and properties to wtFtn (Figures S2B,C, S3, S4A). In contrast to commercial cationized ferritin, which is generated by chemical derivatization of the horse spleen protein with *N*,*N*-dimethyl-1,3-propanediamine,[16] FtnQC12 elutes as a sharp peak from negatively-charged ion-exchange resin (Figure S4B), thus suggesting a more uniform charge distribution. Its later elution time also indicates greater surface charge density compared to chemically cationized ferritin. Although the electrostatic surface potential of wtFtn (Figure 1C) has been suggested to have a funneling effect on the transport of positively charged ions into the ferritin lumen,[17] synthesis of iron oxide nanoparticles inside FtnQC12 proceeded readily and in similar yield as for wtFtn[18] (see the Supporting Information and Figure S5). Efficient mineralization of iron oxide by the supercharged protein was presumably possible because residues in the channels and at the lumenal ferroxidase site were excluded from mutagenesis.

In the absence of guest, AaLS-13 is obtained as a mixture of two quaternary states: fragments (mostly pentamers) and fully assembled capsids.[9b] In the presence of a complementarily charged guest molecule, both states yield cage complexes.[9] To create cage-within-cage structures, we initially explored the ability of supercharged ferritin to template the assembly of AaLS-13 fragments (Figure 2A). The proteins were mixed at neutral pH in buffer containing 200 or 600 mM NaCl at a 4:1 ratio of AaLS-13 to FtnQC12 monomers. This ratio corresponds to approximately two FtnQC12 cages (24 monomers) per AaLS-13 $T=3$ cage (180 monomers). After incubation for 5 days, a significant fraction of the sample had

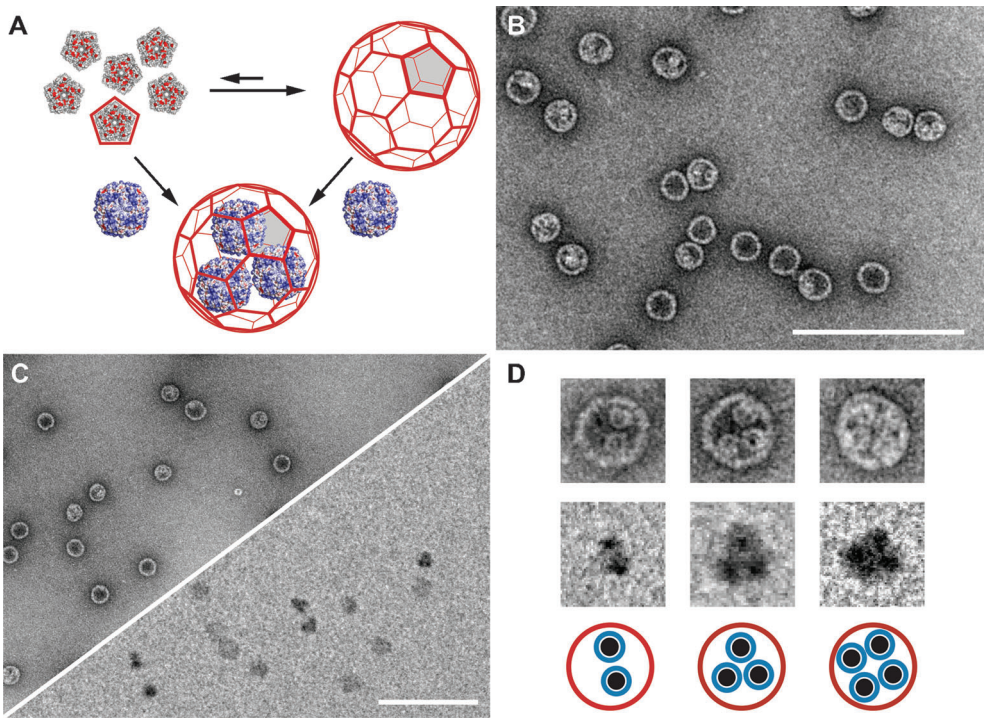

Figure 2. Matryoshka-type assemblies with supercharged ferritin. A) Mixing FtnQC12 (*apo* or *holo*) with AaLS-13 fragments (left) or nanocages (right) in 600 mM NaCl buffer results in encapsulation of the nanocage. B) Electron micrograph of FtnQC12 encapsulated by intact AaLS-13 capsids. Scale bar: 200 nm. C) FtnQC12, loaded with iron oxide nanoparticles, encapsulated by intact AaLS-13 capsids. Sample stained with uranyl acetate (left panel) and without staining agent (right panel). The iron oxide cores form clusters in close proximity, thus indicating localization of the iron-loaded FtnQC12 inside the AaLS-13 nanocage. Scale bar: 200 nm. D) Representative Matryoshka-type supramolecular structures. Top row: Electron micrograph magnifications of AaLS-13 containing two, three, and four supercharged ferritin nanocages. Middle row: Electron micrograph magnifications of iron oxide nanoparticle clusters after Matryoshka-type assembly. Bottom row: Schematic depiction of AaLS-13 nanocages (red circles) with two, three, and four nanocages of supercharged ferritin (blue circles) loaded with iron oxide nanoparticles (black spheres).

been converted to higher-order assemblies, which were isolated by gel filtration and analyzed by negative stain TEM. At low ionic strength (200 mM NaCl), irregular species of sizes that are intermediate between AaLS-13 fragments and assembled nanocages (Figure S6A,B: 16.8 ± 2.1 nm) formed. These complexes likely reflect the non-ordered collapse of negatively charged AaLS-13 fragments onto the positively charged template. By contrast, after 5 days at higher ionic strength (600 mM NaCl), approximately half of the material had assembled into regular closed-shell AaLS-13 nanocages surrounding one or more FtnQC12 guests (Figure S6C). For these closed-shell assemblies, the outer cages had a mean diameter of 30.5 ± 1.6 nm (Figure S6D), which makes them similar in size to capsids assembled from AaLS-13 fragments in control experiments without FtnQC12 (31.7 ± 1.9 nm) but smaller than AaLS-13 capsids preassembled in vivo (34.6 ± 1.6 nm). The loading process appears to follow a Gaussian distribution: less than 3% of the isolated particles were empty, whereas 12% had one guest, 62% two guests, and 23% three guests (Figure S7A). The average loading is two ferritin cages per AaLS-13 nanocage and thus corresponds well to the initial mixing ratio.

When analogous encapsulation experiments were carried out at even higher ionic strength (1M NaCl), the yield of cage-within-cage complexes decreased approximately 10-fold (Figure S8C). Moreover, only complexes containing a single guest molecule were observed. Furthermore, no nested structures were obtained in control experiments with wtFtn (Figure S8E). Together, these results demonstrate that the effective charge on the partner cage proteins strongly influences encapsulation efficiency, thus supporting the hypothesis that the engineered electrostatic interactions provide the driving force for complex formation.

Loading intact AaLS-13 capsids directly with supercharged ferritin is potentially far more challenging than assembly of the host around the guest. Although AaLS-13 capsids have been shown to be highly dynamic, partially disassembling to take up supercharged GFP molecules from solution and then reassembling to generate closed-shell cage complexes with high packing densities,[9b] FtnQC12 is substantially larger than GFP(+36). To test whether objects as large as ferritin can be encapsulated, intact AaLS-13 nanocages were incubated with FtnQC12 at neutral pH in buffer containing 200, 600, or 1000 mM NaCl at a ratio of about two FtnQC12 nanocages per AaLS-13 cage (monomer ratio 4:1). After 5 days, the AaLS-13 fraction was reisolated by gel filtration and analyzed by TEM.

As in the experiments with AaLS-13 fragments, the ionic strength of the incubation buffer proved to be important. Thus, the sample prepared at 200 mM NaCl showed precipitation after mixing; analysis of the supernatant revealed mostly collapsed assemblies of AaLS-13 and FtnQC12 (Figure S9A,B). By contrast, at very high ionic strength (1M NaCl), a few nested cage complexes were observed (Figure S8D). The yield of such structures increased more than 10-fold at 600 mM NaCl, where more than 70% of the FtnQC12 cages were encapsulated within the lumen of regular spherical AaLS-13 capsids (Figure 2B and Figure S9C,D). Although a packing density of 1.4 FtnQC12 per AaLS-13 was obtained, the loading distribution differed from that observed for templated assembly. Roughly 40% of the isolated AaLS-13 particles were empty, 11% contained one FtnQC12 nanocage, 20% two, 23% three, and 4% four guest cages (Figure S7B). The relative abundance of complexes containing multiple ferritins suggests a cooperative loading mechanism. Furthermore, the filled AaLS-13 cages were larger than the assemblages obtained in the templating procedure, with a diameter of 34.7 ± 1.9 nm, but similar in size to the empty cages (34.6 ± 1.6 nm) from the same experiment. These results highlight the remarkable plasticity of the AaLS-13 system. Not only is the AaLS-13 nanocage highly dynamic in solution, and thus capable of engulfing a particle a third of its size through a rapid disassembly–reassembly process, but like wild-type lumazine synthase,[12,13] it can form a range of discretely sized nanoparticles.

Analogous experiments with supercharged ferritin loaded with iron oxide nanoparticles afforded Matryoshka-type structures with three components. The isolated nanocages displayed a strong absorbance at 370 nm in the gel filtration trace (Figure S10A), which is indicative of iron mineral co-eluting with the AaLS-13 cage. TEM analysis of these complexes revealed fully assembled AaLS-13 cages with FtnQC12 as guests (Figure 2C, left panel). Electron micrographs without applied staining agent showed clusters of electron-dense cores (Figure 2C, right panel). Energy-dispersive X-ray spectroscopy proved the presence of iron in the cores (Figure S10B). The distances between these cores were in the range 13 to 20 nm (mean distance 16.1 ± 2.1 nm), which agrees well with the diameter of FtnQC12 and the lumen of AaLS-13 (Figure 2C, right panel). Encapsulation of the iron-loaded FtnQC12 cages within the larger AaLS-13 nanocage thus provides a simple means of spatially organizing several iron oxide nanoparticles in Matryoshka-type structures with two protein layers (Figure 2D).

Our results demonstrate that charge complementarity is well suited to the construction of hierarchically ordered protein assemblies. The final composition of these supramolecular complexes can be tuned by the choice of starting materials (either AaLS-13 cage fragments or intact capsids) and the ionic strength of the incubation buffer. The magnetic properties of iron oxide particles may enable further processing of the obtained assemblies.[19] Given that ferritin has been extensively used as a vessel for the synthesis of structurally diverse composites,[20] a wide range of functionally distinct Matryoshka-type complexes can be envisaged. In principle, it should also be possible to encapsulate mixtures of appropriately charged nanoparticles and/or proteins. Exploiting complementary electrostatic interactions is a potentially general strategy that should be extendable to other protein nanocages to create a variety of nested assemblies with different shapes and sizes. Hierarchically organized cage-within-cage structures based on Coulombic interactions might even be created in vivo. Because the components are genetically encoded, spontaneous in vivo assembly to produce structures analogous to natural protein-bounded reaction chambers in bacteria[6] is conceivable.

Received: August 29, 2014
Revised: September 16, 2014
Published online: November 13, 2014

Keywords: hierarchical structures · nanoparticles · protein engineering · self-assembly · supramolecular chemistry

[1] a) S.-T. Zheng, T. Wu, B. Irfanoglu, F. Zuo, P. Feng, X. Bu, *Angew. Chem. Int. Ed.* **2011**, *50*, 8034 – 8037; *Angew. Chem.* **2011**, *123*, 8184 – 8187; b) S.-T. Zheng, J. T. Bu, Y. Li, T. Wu, F. Zuo, P. Feng, X. Bu, *J. Am. Chem. Soc.* **2010**, *132*, 17062 – 17064.

[2] S. J. Kang, J. B. Kim, C.-Y. Chiu, S. Ahn, T. Schiros, S. S. Lee, K. G. Yager, M. F. Toney, Y.-L. Loo, C. Nuckolls, *Angew. Chem. Int. Ed.* **2012**, *51*, 8594 – 8997; *Angew. Chem.* **2012**, *124*, 8722 – 8725.

[3] a) V. P. Torchilin, *Nat. Rev. Drug Discovery* **2005**, *4*, 145 – 160; b) T.-M. Hsin, E. S. Yeung, *Angew. Chem. Int. Ed.* **2007**, *46*, 8032 – 8035; *Angew. Chem.* **2007**, *119*, 8178 – 8181.

[4] N. P. King, J. B. Bale, W. Sheffler, D. E. McNamara, S. Gonen, T. Gonen, T. O. Yeates, D. Baker, *Nature* **2014**, *510*, 103 – 108.

[5] B. V. V. Prasad, M. F. Schmid in *Viral Molecular Machines*, *Vol. 726* (Eds.: M. G. Rossmann, V. B. Rao), Springer, New York **2012**, pp. 17 – 47.

[6] T. O. Yeates, C. A. Kerfeld, S. Heinhorst, G. C. Cannon, J. M. Shively, *Nat. Rev. Microbiol.* **2008**, *6*, 681 – 691.

[7] a) M. Sutter, D. Boehringer, S. Gutmann, S. Günther, D. Prangishvili, M. J. Loessner, K. O. Stetter, E. Weber-Ban, N. Ban, *Nat. Struct. Mol. Biol.* **2008**, *15*, 939 – 947; b) R. Rahmanpour, T. D. H. Bugg, *FEBS J.* **2013**, *280*, 2097 – 2104.

[8] H. Contreras, M. S. Joens, L. M. McMath, V. P. Le, M. V. Tullius, J. M. Kimmey, N. Bionghi, M. A. Horwitz, J. A. J. Fitzpatrick, C. W. Goulding, *J. Biol. Chem.* **2014**, *289*, 18279 – 18289.

[9] a) B. Wörsdörfer, K. J. Woycechowsky, D. Hilvert, *Science* **2011**, *331*, 589 – 592; b) B. Wörsdörfer, Z. Pianowski, D. Hilvert, *J. Am. Chem. Soc.* **2012**, *134*, 909 – 911.

[10] X. Liu, E. C. Theil, *Acc. Chem. Res.* **2005**, *38*, 167 – 175.

[11] D. M. Lawson, P. J. Artymiuk, S. J. Yewdall, J. M. A. Smith, J. C. Livingstone, A. Treffry, A. Luzzago, S. Levi, P. Arosio, G. Cesareni, *Nature* **1991**, *349*, 541 – 544.

[12] Preassembled AaLS-13 capsids have an external diameter of 35.9 ± 2.5 nm. Although their precise molecular structure is unknown, these values fall within the range previously seen for wild-type and mutant lumazine synthases[13] and are consistent with icosahedral capsids with $T = 3$ or $T = 4$ symmetry (i.e., 180 or 240 identical subunits).

[13] X. Zhang, P. V. Konarev, M. V. Petoukhov, D. I. Svergun, L. Xing, R. H. Cheng, I. Haase, M. Fischer, A. Bacher, R. Ladenstein, W. Meining, *J. Mol. Biol.* **2006**, *362*, 753 – 770.

[14] A. Leaver-Fay, M. Tyka, S. M. Lewis, O. F. Lange, J. Thompson, R. Jacak, K. Kaufman, P. D. Renfrew, C. A. Smith, W. Sheffler, *Methods Enzymol.* **2011**, *487*, 545 – 574.

[15] A. E. Miklos, C. Kluwe, B. S. Der, S. Pai, A. Sircar, R. A. Hughes, M. Berrondo, J. Xu, V. Codrea, P. E. Buckley, *Chem. Biol.* **2012**, *19*, 449 – 455.

[16] D. Danon, L. Goldstein, Y. Marikovsky, E. Skutelsky, *J. Ultrastruct. Res.* **1972**, *38*, 500 – 510.

[17] T. Douglas, D. R. Ripoll, *Protein Sci.* **1998**, *7*, 1083 – 1091.

[18] M. Uchida, M. L. Flenniken, M. Allen, D. A. Willits, B. E. Crowley, S. Brumfield, A. F. Willis, L. Jackiw, M. Jutila, M. J. Young, T. Douglas, *J. Am. Chem. Soc.* **2006**, *128*, 16626 – 16633.

[19] O. Kasyutich, A. Sarua, W. Schwarzacher, *J. Phys. D: Appl. Phys.* **2008**, *41*, 134022 – 134022.

[20] a) N. Gálvez, P. Sánchez, J. M. Domínguez-Vera, A. Soriano-Portillo, M. Clemente-León, E. Coronado, *J. Mater. Chem.* **2006**, *16*, 2757 – 2761; b) Y. J. Kang, M. Uchida, H.-H. Shin, T. Douglas, S. Kang, *Soft Matter* **2011**, *7*, 11078 – 11078; c) B. Hennequin, L. Turyanska, T. Ben, A. M. Beltrán, S. I. Molina, M. Li, S. Mann, A. Patanè, N. R. Thomas, *Adv. Mater.* **2008**, *20*, 3592 – 3596.

